Neurobiology of Disease 158 (2021) 105448

Contents lists available at ScienceDirect

Neurobiology of Disease

journal homepage: www.elsevier.com/locate/ynbdi

Serotonin drives striatal synaptic plasticity in a sex-related manner

Federica Campanelli [a,b,d,1], Gioia Marino [a,b,d,1], Noemi Barsotti [c], Giuseppina Natale [a,b,d], Valeria Calabrese [d,e], Antonella Cardinale [b,e], Veronica Ghiglieri [f], Giacomo Maddaloni [c], Alessandro Usiello [g,h], Paolo Calabresi [b,i], Massimo Pasqualetti [c,j], Barbara Picconi [e,f,*]

[a] Laboratory of Neurophysiology, Santa Lucia Foundation IRCCS, Rome 00143, Italy
[b] Department of Neuroscience, Università Cattolica del Sacro Cuore, Rome 00168, Italy
[c] Department of Biology Unit of Cell and Developmental Biology, University of Pisa, Pisa 56127, Italy
[d] Department of Medicine, Università degli Studi di Perugia, Perugia 06123, Italy
[e] Laboratory Experimental Neurophysiology, IRCCS San Raffaele Pisana, Rome 00166, Italy
[f] Università Telematica San Raffaele, Rome 00166, Italy
[g] Department of Environmental, Biological and Pharmaceutical Sciences and Technologies, University of Campania, Luigi Vanvitelli, Caserta 81100, Italy
[h] IRCCS-Foundation SDN, Via Gianturco, Naples 80143, Italy
[i] Neurologia, Fondazione Policlinico Universitario Agostino Gemelli IRCCS, Rome 00168, Italy
[j] Istituto Italiano di Tecnologia, Center for Neuroscience and Cognitive Systems, Rovereto (TN), 38068, Italy.

ARTICLE INFO

Keywords:
Serotonin
Tph2
Dopamine
Synaptic plasticity
Striatum
Functional recovery

ABSTRACT

Introduction: Plasticity at corticostriatal synapses is a key substrate for a variety of brain functions – including motor control, learning and reward processing – and is often disrupted in disease conditions. Despite intense research pointing toward a dynamic interplay between glutamate, dopamine (DA), and serotonin (5-HT) neurotransmission, their precise circuit and synaptic mechanisms regulating their role in striatal plasticity are still unclear. Here, we analyze the role of serotonergic raphe-striatal innervation in the regulation of DA-dependent corticostriatal plasticity.

Methods: Mice (males and females, 2–6 months of age) were housed in standard plexiglass cages at constant temperature (22 ± 1 °C) and maintained on a 12/12 h light/dark cycle with food and demineralized water ad libitum. In the present study, we used a knock-in mouse line in which the green fluorescent protein reporter gene (GFP) replaced the I *Tph2* exon (*Tph2*^{GFP} mice), allowing selective expression of GFP in the whole 5-HT system, highlighting both somata and neuritis of serotonergic neurons. Heterozygous, *Tph2*$^{+/GFP}$, mice were intercrossed to obtain experimental cohorts, which included Wild-type (*Tph2*$^{+/+}$), Heterozygous (*Tph2*$^{+/GFP}$), and Mutant serotonin-depleted (*Tph2*$^{GFP/GFP}$) animals.

Results: Using male and female mice, carrying on different *Tph2* gene dosages, we show that *Tph2* gene modulation results in sex-specific corticostriatal abnormalities, encompassing the abnormal amplitude of spontaneous glutamatergic transmission and the loss of Long Term Potentiation (LTP) in *Tph2*$^{GFP/GFP}$ mice of both sexes, while this form of plasticity is normally expressed in control mice (*Tph2*$^{+/+}$). Once LTP is induced, only the *Tph2*$^{+/GFP}$ female mice present a loss of synaptic depotentiation.

Conclusion: We showed a relevant role of the interaction between dopaminergic and serotonergic systems in controlling striatal synaptic plasticity. Overall, our data unveil that 5-HT plays a primary role in regulating DA-dependent corticostriatal plasticity in a sex-related manner and propose altered 5-HT levels as a critical determinant of disease-associated plasticity defects.

1. Introduction

Serotonin (5-Hydroxy-Tryptamine, 5-HT) is a widely distributed neuromodulator and neurotransmitter in the brain, involved in the regulation of a broad range of essential physiological functions such as developmental processes, synaptic plasticity, metabolic homeostasis,

* Corresponding author at: Università Telematica San Raffaele, Roma, Lab. Neurofisiologia Sperimentale, IRCCS San Raffaele Pisana, Roma, Italy.
E-mail address: barbara.picconi@uniroma5.it (B. Picconi).
[1] F. Campanelli and G. Marino contributed equally to this work.

https://doi.org/10.1016/j.nbd.2021.105448
Received 12 December 2020; Received in revised form 1 June 2021; Accepted 13 July 2021
Available online 16 July 2021

neuroendocrine function, appetite, energy expenditure, respiratory rate and sleep (Duman et al., 2016). Moreover, the serotonergic system, also through its ability to modulate the activity of other neuronal networks, regulates cognition and complex emotional behaviors, also in its interaction with environmental stress factors (Lesch and Waider, 2012; Svob Strac et al., 2016). Based on this, 5-HT is implicated in a broad spectrum of human behavioral traits, as well as in neurodevelopmental and neuropsychiatric disorders (Heiming et al., 2009). In the Central Nervous System (CNS), tryptophan is hydroxylated to 5-Hydroxy-Tryptophan (5-HTP) by the enzyme tryptophan hydroxylase type 2 (TPH2) that catalyzes the rate-limiting step in 5-HT biosynthesis via its subsequent decarboxylation, which involves the aromatic L-Amino Acid Decarboxylase (AADC) enzyme. Considering the importance of 5-HT in regulating anxiety and depression, preclinical models with partial or complete serotonergic depletion have been used in many studies to investigate the complex role of this neurotransmitter in brain functions (Alenina et al., 2009; Carli et al., 2015; Cervo et al., 2005; Maddaloni et al., 2017; Pratelli and Pasqualetti, 2019; Zhang et al., 2004).

Mouse molecular genetics experiments overall demonstrated that lack of 5-HT leads to a drastic reduction in the body growth rate, a high lethality rate and, most importantly, produces severe abnormalities in the serotonergic circuitry formation with brain region- and time-specific effects (Alenina et al., 2009). Among the different animal models with altered serotonergic transmission, Pasqualetti and colleagues in 2013 developed a knock-in (*Tph2*^{GFP}) animal model by the introduction of the enhanced green fluorescent protein (eGFP) into the *Tph2* locus in a way to highlight the serotonergic neurons independently of 5-HT immunoreactivity (Migliarini et al., 2013). Intriguingly, besides the apparently normal distribution observed in the cortex and the striatum, the development of 5-HT axon terminal arborization exhibited, as a consequence of *Tph2* inactivation, a diametrically opposite response in distinct brain areas (Migliarini et al., 2013).

To date, the interaction between serotonergic and dopaminergic systems is still under investigation. Many studies conducted so far claim an involvement of the 5-HT system in the modulation of the activity of dopaminergic neurons and in the regulation of corticostriatal synaptic transmission (De Deurwaerdere and Di Giovanni, 2017; Ogawa and Watabe-Uchida, 2018). The 5-HT afferents arising from the dorsal raphe nucleus innervate all components of the basal ganglia circuitry (Cavaccini et al., 2018). In 2004, Trudeau and collaborators proposed that all, or a subset of, axon terminals established by monoamine neurons might contain and release glutamate in addition to dopamine (DA) or 5-HT (Trudeau, 2004). These findings proved that there is a unique monoaminergic mechanism controlling presynaptic inhibition of corticostriatal glutamate release and, in turn, prompted to investigate how DA and 5-HT systems may interact to influence striatum-dependent processes. This view is supported by the discovery that the raphe neurons, the main source of serotonergic fibers that project to almost all regions of the brain, are immunoreactive for glutamate and vesicular glutamate transporter 3 (VGLUT3) (Gras et al., 2002; Nicholas et al., 1992; Ottersen and Storm-Mathisen, 1984) as well as phosphate-activated glutaminase, an enzyme involved in the glutamate metabolism (Kaneko et al., 1990).

Herein, we investigated the involvement of 5-HT in corticostriatal synaptic plasticity of striatal projection neurons (SPNs) recorded from male and female *Tph2* knock-in mutant mice (*Tph2*$^{GFP/GFP}$), which are depleted of brain 5-HT. Using an array of in vitro electrophysiological paradigms, we found sex-dependent abnormalities in corticostriatal plasticity, indicating a previously unappreciated sex-related role of 5-HT in the modulation of corticostriatal synapses and a relevant role of serotonergic interplay in modulating glutamatergic synaptic activity within the striatal nucleus. In addition, the electrophysiological recordings of SPNs from 6-hydroxydopamine (6-OHDA)-lesioned *Tph2*^{GFP} mice allowed us to identify a possible serotonergic involvement also in a pathological condition involving DA as the main neurotransmitter.

2. Materials and methods

2.1. Animals

Mice (males and females, 2–6 months of age) were housed in standard plexiglass cages at constant temperature (22 ± 1 °C) and maintained on a 12/12 h light/dark cycle, with food and demineralized water ad libitum. All experiments were approved by the European Communities Council Directive of September 2010 (2010/63/E), and by the Veterinary Department of the Italian Ministry of Health (protocol No. 1296/2015PR).

In the present study, we used the *Tph2*^{GFP} allele described in Migliarini et al., 2013 in which the first exon of the *Tph2* gene was replaced by the reporter gene GFP, abolishing the expression of the rate-limiting enzyme of 5-HT synthesis. *Tph2*^{GFP} mice display selective expression of the green fluorescent reporter gene in the whole 5-HT system, highlighting both somata and neuritis of serotonergic neurons. Heterozygous mice, *Tph2*$^{+/GFP}$, were intercrossed to obtain pups that were genotyped, as previously reported (Migliarini et al., 2013). The experimental cohorts included Wild-type (*Tph2*$^{+/+}$), Heterozygous (*Tph2*$^{+/GFP}$), and Mutant serotonin-depleted (*Tph2*$^{GFP/GFP}$) animals.

2.2. Serotonin fiber analysis

Immunohistochemistry. Animals were deeply anesthetized and perfused transcardially with PBS followed by 4% paraformaldehyde (PFA). Brains were dissected out and post-fixed overnight (o/n) at 4 °C in 4% PFA before being sectioned with a vibratome (Leica Microsystem) to obtain 50-μm-thick coronal sections. To obtain striatal serotonin transporter (SERT) immunostaining, sections were incubated 48 h at 4 °C with primary antibody rabbit anti-SERT (1:500, Millipore, ab9726) in PB-Triton 0.3% and horse serum 5%. Sections were rinsed in PB-Triton 0.3% and then incubated with secondary antibody Alexa Fluor 594 anti-rabbit (1:500, ThermoFisher Scientific, R6394). Sections were eventually mounted on slides for microscope analysis. Control sections were processed in parallel, but the primary antibody was omitted.

For GFP labeling, 50 μm brain sections were then incubated o/n at 4 °C with the primary antibody chicken anti-GFP (1:1000, Abcam, ab13970). After washes in PB-Triton 0.5% sections were incubated overnight at 4 °C with the secondary antibody Alexa Fluor 488 goat anti-chicken IgG (1:500, Life Technologies, A11039).

Image acquisition and analysis. Images of SERT immunostaining were acquired with a confocal microscope Nikon A1. For three animals of each genotype, five sections were chosen at comparable antero-posterior localization and imaged. For each section, a series of 15 optical plans (z-step 0.8 μm, for a total 10 μm thickness) was acquired with a 20× plan-apochromat objective numerical aperture NA = 0.75, and confocal fluorescence filter 595/50.

Quantification of fluorescence intensity (optical density, OD) was measured using the ImageJ software. To obtain relative optical density value (ROD), background value measured on control sections was subtracted to the OD value. Statistical significance was tested with GraphPad Prism 6 software using one-way Anova with Multiple comparisons and Bonferroni's correction.

For GFP-positive serotonergic fibers images, three high power images were acquired on each of 3 consecutive sections with a 60× plan-apochromat objective, numerical aperture NA = 1.4 (69 stacks with a 0.15 μm step and 1024 × 1024 pixels resolution, for a pixel size of 0.21 μm), and confocal fluorescence filter 525/50. For each picture, 3D-reconstruction analysis was performed on three blocks of 300 pixels × 300 pixels × 68 stacks (xyz: 63 μm × 63 μm × 10 μm = 39.69 × 10^3 μm^3) using the semi-automatic Filament tool of Imaris software (Bitplane). Each block analyzed was manually corrected for false segments, then dendrite volume, dendrite length, edge diameter values have been extracted from IMARIS output and plotted with GraphPad Prism 6.0 software (Maddaloni et al., 2017). Twenty-seven blocks per animal have

been averaged to generate a group mean and SEM ($n = 3$ mice per genotype). For the tortuosity parameter, single fibers have been reconstructed and the total length has been measured (15 fibers per animal, $n = 3$ mice). Tortuosity index was calculated as the Dendrite length/Euclidean distance ratio between the ends of the fiber (Pratelli et al., 2017). Statistical significance was calculated with a Two-Tailed *Student's t-test* for unpaired data with GraphPad Prism 6.0 software.

2.3. Electrophysiology

Tph2 mice (Male: $Tph2^{+/+}$, $n = 11$, $Tph2^{+/GFP}$, $n = 6$, $Tph2^{GFP/GFP}$, $n = 4$; Female: $Tph2^{+/+}$, $n = 8$, $Tph2^{+/GFP}$, $n = 9$, $Tph2^{GFP/GFP}$, $n = 4$) were used for all the electrophysiological experiments. Before all recordings in female mice the stage of estrous cycle was determinate (proestrus, estrus, metestrus, and diestrus) by visual observation as described in literature (Byers et al., 2012). Diestrus rather than metestrus was chosen to ensure that mice were completely out of the estrus phase.

Electrophysiology recordings were used to study the intrinsic membrane properties and synaptic plasticity of SPNs in corticostriatal slices. The animals were initially anesthetized with 2-Bromo-2-Chloro-1,1,1-Trifluoroethane (Sigma) and then sacrificed by cervical dislocation. Corticostriatal coronal slices were cut from *Tph2* mouse brains (thickness, 240 μm for patch-clamp and 280 μm for intracellular) using a vibratome (Leica VT 1200S) and have been preserved in the artificial cerebral spinal fluid (ACSF) in constant oxygenation, which composition was (in mM): 126 NaCl, 2.5 KCl, 1.2 $MgCl_2$, 1.2 NaH_2PO_4, 2.4 $CaCl_2$, 10 glucose and 25 $NaHCO_3$. A single slice was transferred to a recording chamber and submerged in a continuously flowing Krebs' solution (RT; 2.5–3 ml/min), bubbled with a 95% O_2–5% CO_2 gas mixture.

2.3.1. Intracellular recordings with sharp electrodes

Signals were recorded with the use of an Axoclamp 2B amplifier (Molecular Devices), displayed on a separate oscilloscope, stored, and analyzed on a digital system (pClamp 9, Molecular Devices). Bipolar tungsten stimulating electrode (76 mm, 3 μm, 0.1 MΩ, World Precision Instruments) was connected to a stimulation unit (Grass Telefactor) and placed within the corpus callosum. Recording sharp electrodes were pulled from borosilicate glass pipettes filled with 2 M KCl (30–60 MΩ). Glutamatergic excitatory postsynaptic potentials (EPSPs) were evoked every 10 s and, to induce Long Term Depression (LTD) and Long Term Potentiation (LTP), a High Frequency Stimulation (HFS) protocol was used, consisting of three trains of 100 Hz, 3 s of duration and 20 s of interval. During tetanic stimulation, the intensity was increased to suprathreshold levels. For the LTP protocol, at the beginning of intracellular recordings, magnesium ions were omitted from the medium to increase the *N*-methyl-D-aspartate (NMDA)-mediated component of EPSP (Calabresi et al., 1992). To study depotentiation of previously induced LTP, a Low-Frequency Stimulation (LFS) (2 Hz frequency for 10 min) has been applied 10 min after LTP induction (Ghiglieri et al., 2015; Martella et al., 2009; Picconi et al., 2003). Current-voltage relationships were obtained by applying steps of current of 200 pA in both hyperpolarizing and depolarizing direction (from −400 to +200 pA) to measure the membrane ability to accommodate and fire in response to hyperpolarizing and depolarizing current steps. Firing frequency was calculated as the mean number of spikes in response to a step of 500 pA in 500 ms and shown as average in whisker plots (Fig. 2A–F).

2.3.2. Whole-cell patch-clamp recordings

SPNs were also recorded in whole-cell patch-clamp configuration from corticostriatal slices using borosilicate glass electrodes BF150–86-10 (1.8 mm OD, 0.86 mm ID, length 10 cm) pulled on a P-1000 Puller (Sutter Instruments). Pipette resistances ranged from 3.5 to 5 MΩ. The electrodes were filled with the following intracellular solution (in mM): K-D-gluconate 120, KCl 20, EGTA (Ethylene glycol-bis-N-tetracetic acid) 0.2, Hepes acid (N-2-hydroxyethylpiperazine-N-2-ethanesulfonic acid) 10, $MgCl_2$ 2, Mg_2ATP 4, NaGTP 0.4. Recordings were made with a Multiclamp 700B amplifier (Molecular Devices), with an infrared differential interference contrast microscopy to visualized SPNs in dorsal striatum (Eclipse FN1, Nikon) (Bagetta et al., 2012; Cerovic et al., 2015). Membrane currents and access resistance (range of 10–30 MΩ before electronic compensation) were continuously monitored. A bipolar stimulant was placed in the white matter between the cortex and the striatum to evoke glutamate-mediated synaptic currents in the neuronal population, while the recording electrodes were placed within the dorsolateral striatum. During the experiment input resistances and injected currents were monitored. Variations of these parameters >20% lead to the rejection of the experiment. Data from the neuronal activity were collected and analyzed using Clamp 10. EPSP modifications induced by HFS are expressed as a percentage of control, the latter representing the mean of responses recorded during a stable period (10 min before the tetanus) (Ghiglieri et al., 2015). For spontaneous excitatory postsynaptic currents (sEPSCs), patch-clamp electrodes were filled with intracellular solution, mentioned above. Cells were clamped at the holding potential (HP) of −70 mV. The striatal synaptic plasticity has been induced through the same experimental protocols described in the above paragraph.

Both patch-clamp and intracellular recordings with sharp electrodes were used for intrinsic membrane properties and synaptic plasticity experiments. When results were similar, and the extent of changes comparable, normalized values obtained from the two approaches were pooled and plotted together. Differently, the spontaneous glutamatergic transmission was recorded using only the whole-cell patch-clamp technique. All the experiments have been conducted in the continuous presence of 50 μM Picrotoxin to avoid GABA transmission.

Values given in the text and in the figures are presented as mean ± SEM of changes in the respective cell populations. Statistical comparisons between different experimental groups were analyzed using a one- or two-way ANOVA, to highlight the possible interactions. If these values were significantly different, $P < 0.05$, the tests were followed by Bonferroni's test for post-hoc comparison. Student's *t*-test was used for the analysis of the pre- versus post-HFS protocol in the same cell population and to compare the spikes frequency and the spontaneous activity of the different experimental groups. Current-voltage (I-V) curves were compared using ANOVA. The analyses were done using Prism 6.0 software (GraphPad Software).

2.4. Unilateral intrastriatal 6-OHDA experimental model of Parkinson's disease

$Tph2^{+/+}$ ($n = 8$) and $Tph2^{+/GFP}$ ($n = 8$) females and males mice have been deeply anesthetized with a 10 ml/kg solution contents 500 μL of Zoletil (5 mg/kg, i.p., Virbac S.r.l., Milan, Italy) and 500 μL di Rompum (9 mg/kg, i.p., Bayer S.p.A., Italy) and unilaterally injected via a Hamilton syringe with 8 μg/4 μL 6-OHDA (Sigma Aldrich AB) in saline 0.1% ascorbic acid into the striatum at a rate of 0.38 μL/min at the following coordinates (in mm) relative to bregma and the dural surface: anteroposterior (AP) = +1.0, medio-lateral (ML) = +1.8, dorso-ventral (DV) = −2.9. This intrastriatal 6-OHDA injection lesion was associated with a success rate of only 14% (this parameter includes an 82% post-operative mortality and significant DA depletion in 78% of the surviving animals) (Lundblad et al., 2004). Considering these data, we did not include the group of $Tph2^{GFP/GFP}$ mice in this characterization. In fact, because of their low post-operative survival, we could not obtain the right number of mice to perform reliable electrophysiological recordings (Fig. 6A). Fifteen days later, 6-OHDA-lesioned mice were challenged for spontaneous rotations. However, in our hands, the very low tyrosine hydroxylase (TH) % loss did not allow us to appreciate good spontaneous turning behavior. Thus, monitoring of the lesion extent has been performed after recordings by immunofluorescence analysis. Electrophysiological experiments were performed 1 month after the lesion.

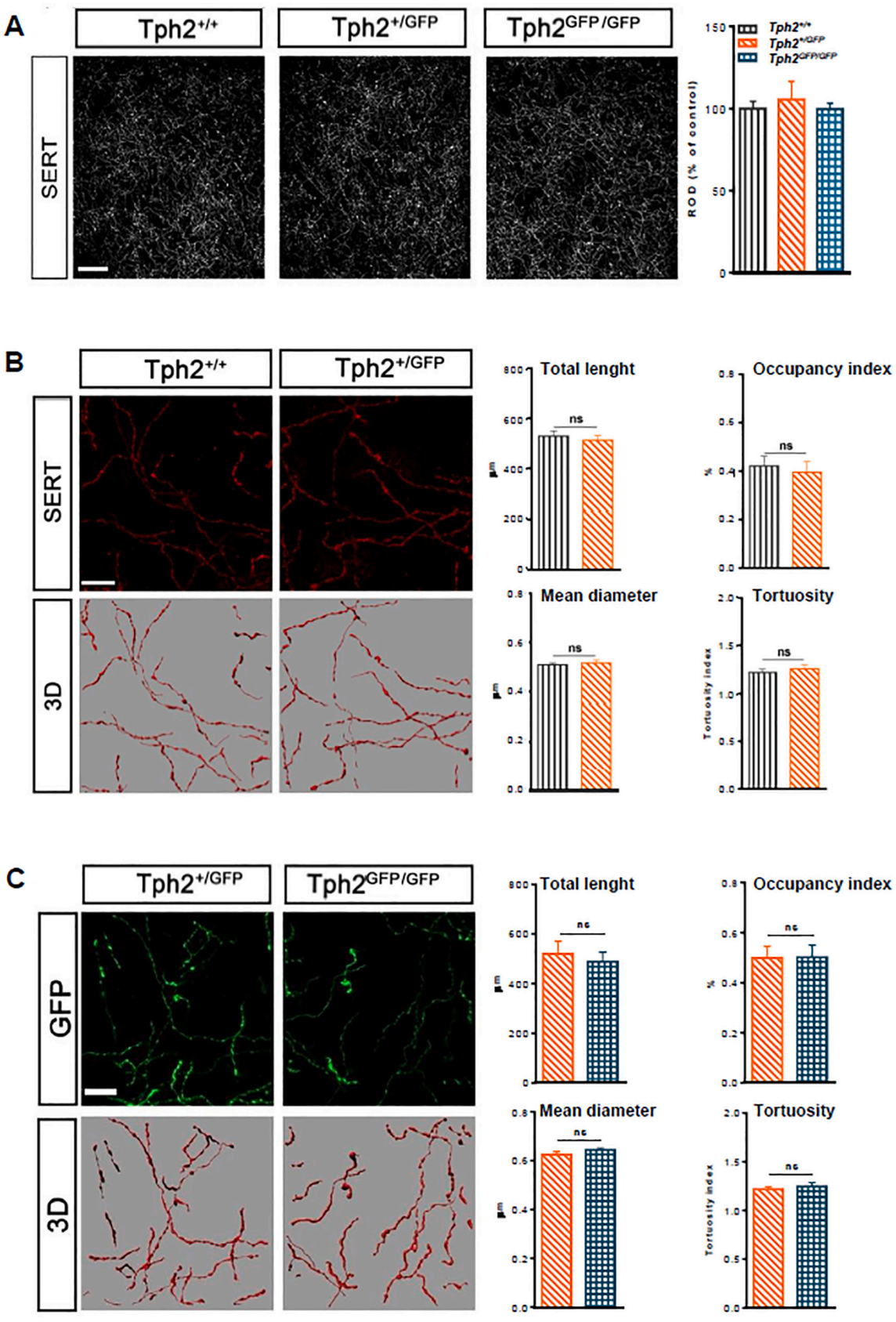

(caption on next page)

Fig. 1. Analysis of serotonergic innervation in the striatum of mice depleted of brain serotonin. A) Representative images of SERT immunolabeling in the striatum of *Tph2*$^{+/+}$, *Tph2*$^{+/GFP}$, *Tph2*$^{GFP/GFP}$ mice. Quantification of ROD measurements of 5-HT innervation density was plotted as a bar graph. Data were presented as percentage compared to control (mean ± SEM) ($n = 3$ mice per genotype) ($P > 0.05$). Scale bar: 100 μm. B) Representative high power confocal images of SERT- (red) striatal serotonergic fibers, and their 3D-reconstructions performed in *Tph2*$^{+/+}$, *Tph2*$^{+/GFP}$ and *Tph2*$^{GFP/GFP}$ mice (Scale bar: 10 μm). Bar graphs show total length, mean diameter, occupancy index (volume occupied by the 5-HT fibers in the analyzed block expressed as percentage) and tortuosity of the striatal serotonergic axons analyzed in each genotype. Data are shown as mean ± SEM ($P > 0.05$, $n = 3$ per genotype). C) Representative high-power confocal acquisition of GFP-immunoreactive serotonergic fibers (green) and computer-based 3D reconstructions (red) in *Tph2*$^{+/GFP}$ and *Tph2*$^{GFP/GFP}$ mice. Total length, mean diameter, occupancy index (total volume of analyzed block occupied by 5-HT fibers expressed as percentage), and tortuosity parameter of 5-HT fibers were analyzed. Graphs show data as mean ± SEM ($P > 0.05$) ($n = 3$ mice per genotype). Scale bar: 10 μm. (For interpretation of the references to colour in this figure legend, the reader is referred to the web version of this article.)

2.5. Immunohistochemistry

Anesthetized mice were perfused transcardially using 0.9% saline and 4% paraformaldehyde solution. Whole brains were post-fixed overnight in 4% paraformaldehyde and then moved to a 30% sucrose solution with 0.02% of sodium azide to avoid contamination. Next, brains were cut into 30 μm thick sections using a cryostat (LEICA) and stored sequentially in 0.1 M PB pH 7.4 solution, containing 0.02% of sodium azide (free-floating). The selected sections (approximately 7/8 sections per animal, $n = 4$) were incubated with rabbit anti-TH primary antibody in PB-Triton X 100 0.3% for 3 O/N at 4 °C (1: 1000 – Merck Millipore AB152). After incubation with the appropriate secondary antibody (Cy3 donkey anti-rabbit, 1:200, The Jackson Immunoresearch 711–165-152), the sections were mounted on coverslips through an aqueous Gel-Mount ™ solution (Sigma-Aldrich). The images were acquired under a Nikon Confocal Microscope (NIKON T*i*E2 equipped with standard filter sets for TRITC (570/620 nm)), with a 20× objective (N. A. = 0.50), and using the LARGE IMAGE Acquisition. During the acquisitions, all parameters were kept constants for all groups. Densitometric analysis of TH immunoreactivity in the dorsolateral region of the striatum was performed off-line on confocal images with Fiji software (Schindelin et al., 2012) and expressed as a percentage compared to the contralateral side. Quantification was done on 7/8 regularly spaced sections (*Tph2*$^{+/+}$$n = 4$ and*Tph2*$^{+/GFP}$ $n = 4$, mice both sexes).

3. Results

3.1. Serotonergic fibers are unaffected in the striatum of mice depleted of brain serotonin

Based on the evidence that fluctuations of 5-HT levels in the hippocampal serotonergic projections are associated with increased plasticity such as a marked hyperinnervation (Migliarini et al., 2013), we first studied the striatal organization of the 5-HT fibers in animals depleted of 5-HT. We performed an immunohistochemical analysis against the 5-HT transporter SERT in Wild-type (*Tph2*$^{+/+}$), heterozygous (*Tph2*$^{+/GFP}$) and Mutant (*Tph2*$^{GFP/GFP}$) adult animals (Fig. 1A). Quantitative analysis showed that the density of serotonergic innervation was comparable among the three genotypes, as assessed by relative optical density (ROD) measurement (Fig. 1A). Moreover, we wanted to further characterize the striatal serotonergic fibers in order to confirm that in this brain district the serotonergic wiring is not affected by fluctuations of 5-HT levels. To this aim we generated 3D reconstructions for a quantitative computer-based evaluation of total length, mean diameter, volume (occupancy index) and tortuosity of serotonergic fibers for the three genotypes *Tph2*$^{+/+}$, *Tph2*$^{+/GFP}$ and *Tph2*$^{GFP/GFP}$ (Fig. 1B, C). 3D reconstructions from high-magnification confocal image acquisitions of SERT immunostained striatal sections showed no significant differences for any of the parameters analyzed in *Tph2*$^{+/GFP}$ as compared to *Tph2*$^{+/+}$ control mice (Fig. 1B). For the analysis of the serotonergic fibers in animals depleted of brain 5-HT we took advantage of the *Tph2*^{GFP} -knock-in mouse line and generated 3D reconstructions of GFP-immunoreactive axons from high-magnification confocal images of GFP-labeled 5-HT fibers in the striatum of *Tph2*$^{+/GFP}$ and *Tph2*$^{GFP/GFP}$ mice (Fig. 1C). Results showed comparable total length, mean diameter, volume, and tortuosity of 5-HT fibers between *Tph2*$^{+/GFP}$ and *Tph2*$^{GFP/GFP}$ mice in the striatum (Fig. 1C). Overall, these analyses showed that serotonergic fibers are unaffected in the striatum of mice depleted of brain 5-HT, and allowed us to exclude any gross morphological rearrangements as an underlying factor in future analyses.

3.2. Altered serotonergic homeostasis does not affect intrinsic membrane properties of striatal projection neurons, both in male and female mice

We assessed whether partial or total *Tph2* gene inactivation may affect the intrinsic membrane and firing properties of SPNs and their ability to express synaptic plasticity. Electrophysiological recordings from SPNs in all experimental groups, *Tph2*$^{+/+}$, *Tph2*$^{+/GFP}$ and *Tph2*$^{GFP/GFP}$ from both male and female mice, showed similar discharge firing patterns (Fig. 2A and D), and resting membrane potential (RMP), calculated at 0 pA from the I-V curve (Fig. 2B, male: *Tph2*$^{+/+} = 10$ mice, -84.12 ± 0.47 mV; *Tph2*$^{+/GFP} = 6$ mice, -85.44 ± 0.65 mV; *Tph2*$^{GFP/GFP} = 4$ mice, -85.51 ± 3.14 mV; Fig. 2E, female: *Tph2*$^{+/+} = 8$ mice, -84.82 ± 1.03 mV; *Tph2*$^{+/GFP} = 9$ mice, -86.13 ± 0.68 mV; *Tph2*$^{GFP/GFP} = 4$ mice, -85.38 ± 1.56 mV). The measure of the mean number of spikes was found similar between sexes in physiological condition (male: *Tph2*$^{+/+} = 5$ mice, $n = 5$ cells, 16.36 ± 0.86; female: *Tph2*$^{+/+} = 4$ mice, $n = 4$ cells, 16.00 ± 1.63) (Fig. 2C and F). Partial (*Tph2*$^{+/GFP}$) or complete (*Tph2*$^{GFP/GFP}$) inactivation of the *Tph2* gene responsible for the rate-limiting step for the synthesis of 5-HT did not cause any alteration in the intrinsic properties of the neurons, as the firing discharge (Fig. 2A and D), the spiking frequency (male: *Tph2*$^{+/GFP} = 6$ mice, $n = 7$ cells, 15.16 ± 1.10; *Tph2*$^{GFP/GFP} = 4$ mice, $n = 4$ cells, 16.33 ± 1.84; female: *Tph2*$^{+/GFP} = 9$ mice, $n = 11$ cells, 15.66 ± 0.76; *Tph2*$^{GFP/GFP} = 3$ mice, $n = 3$ cells, 17.67 ± 0.88) (Fig. 2C, Students' *t*-test, males, *Tph2*$^{+/+}$ vs *Tph2*$^{+/GFP}$: $t = 0.79$, $df = 10$; *Tph2*$^{+/+}$ vs *Tph2*$^{GFP/GFP}$: $t = 0.015$, $df = 7$; *Tph2*$^{+/GFP}$ vs *Tph2*$^{GFP/GFP}$: $t = 0.58$, $df = 9$, $P > 0.05$ for all groups; Fig. 2F, Students' *t*-test, females, *Tph2*$^{+/+}$ vs *Tph2*$^{+/GFP}$: $t = 0.28$, $df = 13$; *Tph2*$^{+/+}$ vs *Tph2*$^{GFP/GFP}$: $t = 1.29$, $df = 7$; *Tph2*$^{+/GFP}$ vs *Tph2*$^{GFP/GFP}$: $t = 1.29$, $df = 12$, $P > 0.05$ for all groups) and the current–voltage relationship, expressing the capacity of the membrane to respond to current steps of increasing intensity (hyperpolarizing and depolarizing current steps from −400 pA to +200 pA), as compared to the *Tph2*$^{+/+}$ group (Fig. 2B, one-way ANOVA Bonferroni's multiple comparisons, males, $F_{(2,18)} = 0.024$, $P > 0.05$; *Tph2*$^{+/+}$, $n = 21$ cells, vs *Tph2*$^{+/GFP}$, $n = 11$ cells: $t = 0.13$, $df = 18$; *Tph2*$^{+/+}$ vs *Tph2*$^{GFP/GFP}$, $n = 7$ cells: $t = 0.09$, $df = 18$; *Tph2*$^{+/GFP}$ vs *Tph2*$^{GFP/GFP}$: $t = 0.22$, $df = 18$; Fig. 2E, one-way ANOVA, females, $F_{(2,18)} = 0.010$, $P > 0.05$; *Tph2*$^{+/+}$, $n = 12$ cells, vs *Tph2*$^{+/GFP}$, $n = 19$ cells: $t = 0.023$, $df = 18$; *Tph2*$^{+/+}$ vs *Tph2*$^{GFP/GFP}$, $n = 6$ cells: $t = 0.11$, $df = 18$; *Tph2*$^{+/GFP}$ vs *Tph2*$^{GFP/GFP}$: $t = 0.13$, $df = 18$).

3.3. Role of serotonergic tone on spontaneous glutamatergic activity in *Tph2*$^{GFP/GFP}$ mice

To evaluate if the lack of 5-HT impacts on corticostriatal glutamatergic transmission, we examined sEPSCs in SPNs in the three genotypes using whole-cell patch-clamp recordings. As reported in Fig. 2G and H, glutamatergic transmission, in terms of amplitude of sEPSCs, is significantly increased in *Tph2*$^{GFP/GFP}$ (4 males and 4 females) mice from both sexes as compared with *Tph2*$^{+/+}$ (5 males and 5 females) and

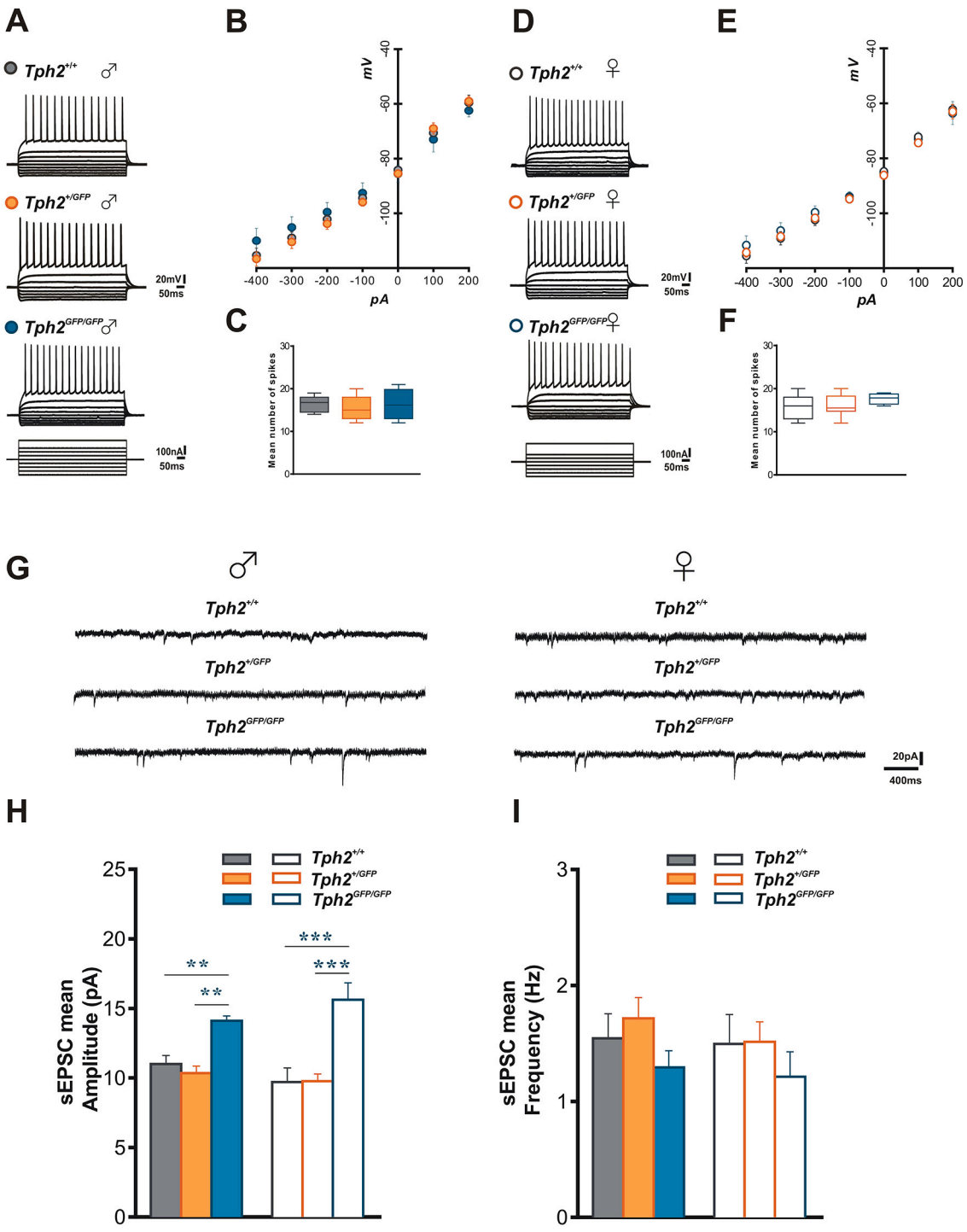

Fig. 2. Intrinsic membrane properties of striatal projection neurons (SPNs) and spontaneous glutamatergic activity. A, D) The analysis of the firing discharge of SPNs recorded from the six different experimental groups. Different content of 5-HT of *Tph2*$^{+/GFP}$ and *Tph2*$^{GFP/GFP}$ mice versus *Tph2*$^{+/+}$ does not alter the action potential discharge induced by depolarizing current steps in SPNs (A, D). B, E) current-voltage (I-V) curves from recordings in dorsolateral striatum were found similar in all the experimental conditions, in both male and female mice. C, F) Comparative graph of the firing spike number between the various *Tph2*$^{+/+}$, *Tph2*$^{+/GFP}$ and *Tph2*$^{GFP/GFP}$ groups. G) Representative traces of spontaneous activity recorded from the two sexes. H) Amplitude and I) frequency of spontaneous excitatory postsynaptic currents (sEPSCs) glutamatergic transmission in *Tph2*$^{+/+}$, *Tph2*$^{+/GFP}$ and *Tph2*$^{GFP/GFP}$ mice, both males and females. The amplitude (H) of sEPSC is increased in *Tph2*$^{GFP/GFP}$ mice, sex-independently, compared to *Tph2*$^{+/+}$ mice. One-way ANOVA: interaction x genotypes, Bonferroni post-hoc $F_{(2,19)} = 8.329$, *Tph2*$^{+/+}$, $n = 9$ cells, vs *Tph2*$^{GFP/GFP}$, $n = 4$ cells, males, $^{**}P < 0.01$, *Tph2*$^{+/GFP}$, $n = 9$ cells, vs *Tph2*$^{GFP/GFP}$, $n = 4$ cells, males, $^{**}P < 0.01$, *Tph2*$^{+/+}$, $n = 9$ cells, vs *Tph2*$^{+/GFP}$, $n = 9$ cells, males, ns $P > 0.05$; $F_{(2,18)} = 13.73$, *Tph2*$^{+/+}$, $n = 5$ cells, vs *Tph2*$^{GFP/GFP}$, $n = 4$ cells, females, $^{***}P < 0.001$, *Tph2*$^{+/GFP}$, $n = 12$ cells, vs *Tph2*$^{GFP/GFP}$, $n = 4$ cells, females, $^{***}P < 0.001$, *Tph2*$^{+/+}$, $n = 5$ cells, vs *Tph2*$^{+/GFP}$, $n = 12$ cells, females, ns $P > 0.05$.

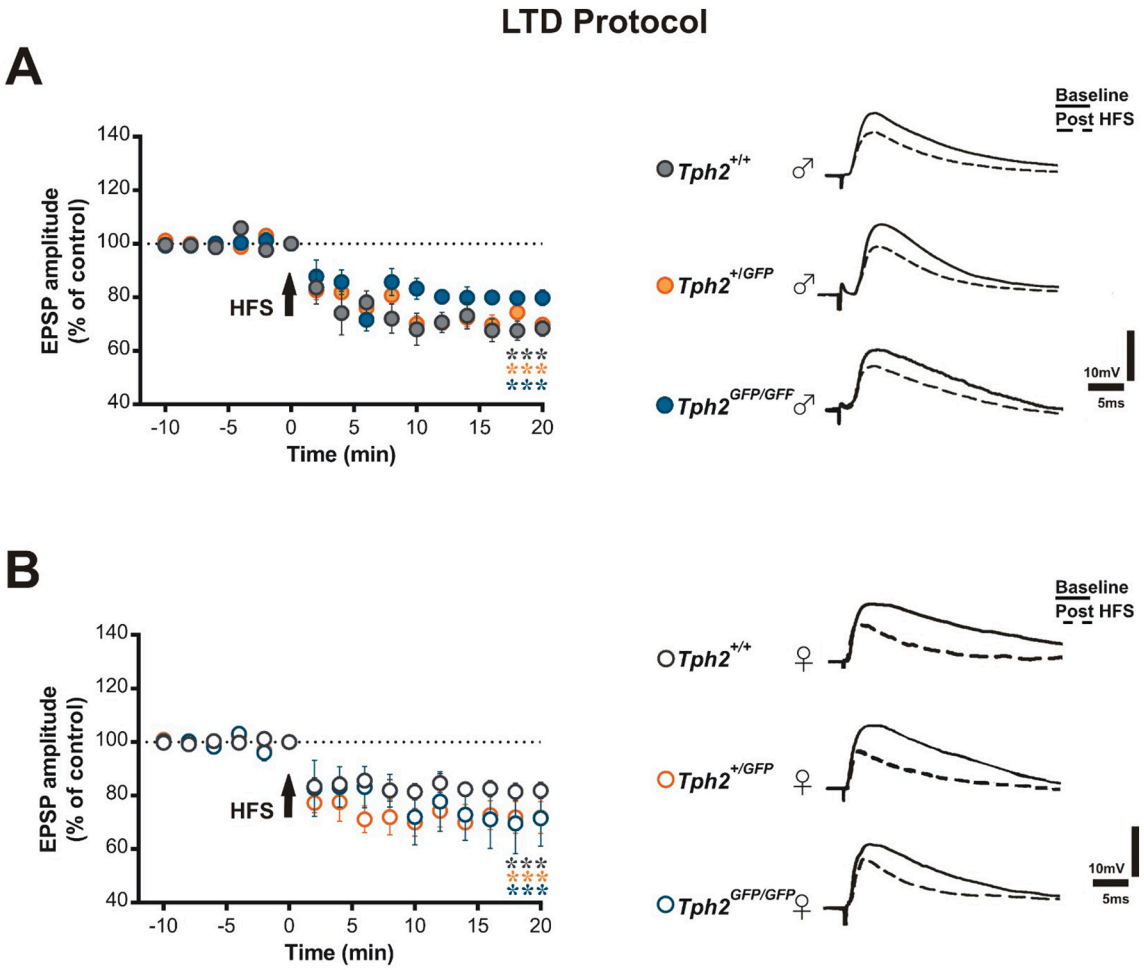

Fig. 3. Long Term Depression (LTD) is normally expressed in all groups. Time-course plots of excitatory postsynaptic potential (EPSP) amplitude (left) and pairs of traces (right) show that high frequency stimulation (HFS) of corticostriatal fibers was able to induce persistent LTD of evoked EPSP in all experimental groups. A) males pre vs 20 min post HFS, Mann-Whitney test, $Tph2^{+/+}$, $n = 7$ cells, $Tph2^{+/GFP}$, $n = 6$ cells, $Tph2^{GFP/GFP}$, $n = 4$ cells, $^{***}P < 0.0001$ for all groups; B) females pre vs 20 min post HFS, Mann-Whitney test, $Tph2^{+/+}$, $n = 7$ cells, $Tph2^{+/GFP}$, $n = 7$ cells, $Tph2^{GFP/GFP}$, $n = 4$ cells, $^{***}P < 0.001$ for all groups.

$Tph2^{+/GFP}$ (6 males and 8 females) mice of the respective sex (Fig. 2H; one-way ANOVA, Bonferroni post-hoc: $F_{(2,19)} = 8.329$, $Tph2^{+/+}$, $n = 9$ cells, vs $Tph2^{GFP/GFP}$, $n = 4$ cells, males, $^{**}P < 0.01$,$Tph2^{+/GFP}$, $n = 9$ cells, vs $Tph2^{GFP/GFP}$, $n = 4$ cells, males, $^{**}P < 0.01$,$Tph2^{+/+}$, $n = 9$ cells, vs $Tph2^{+/GFP}$, $n = 9$ cells, males, $P > 0.05$; $F_{(2,18)} = 13.73$, $Tph2^{+/+}$, $n = 5$ cells, vs $Tph2^{GFP/GFP}$, $n = 4$ cells, females, $^{***}P < 0.001$, $Tph2^{+/GFP}$, $n = 12$ cells, vs $Tph2^{GFP/GFP}$, $n = 4$ cells, females, $^{***}P < 0.001$, $Tph2^{+/+}$, $n = 5$ cells, vs $Tph2^{+/GFP}$, $n = 12$ cells, females, $P > 0.05$). Conversely, the frequency of sEPSCs is comparable in SPNs of all genotypes (Fig. 2I). These data indicate that the lack of 5-HT causes an alteration in glutamatergic transmission mainly at the postsynaptic level, and therefore in the mechanisms undergoing the synaptic plasticity.

3.4. Corticostriatal synaptic plasticity alterations in Tph2 mice

To evaluate the effects of 5-HT absence on long-term striatal synaptic plasticity, we performed a protocol that induces the DA-dependent LTD in the dorsolateral striatum (Calabresi et al., 1992). Whole-cell patch-clamp and sharp-electrode recordings showed that SPNs were capable to express a normal decrease of EPSPs amplitude (LTD) 20 min after tetanic stimulation in all three genotypes, both in males and females (Male mice: $Tph2^{+/+}$, $n = 4$, $Tph2^{+/GFP}$, $n = 4$, $Tph2^{GFP/GFP}$, $n = 3$; Female mice: $Tph2^{+/+}$, $n = 3$, $Tph2^{+/GFP}$, $n = 4$, $Tph2^{GFP/GFP}$, $n = 3$) (Fig. 3A, males pre vs 20 min post HFS: Mann-Whitney test, $Tph2^{+/+}$, $n = 7$ cells; $Tph2^{+/GFP}$, $n = 6$ cells; $Tph2^{GFP/GFP}$, $n = 4$ cells: $^{***}P < 0.0001$ for all groups; Fig. 3B, females pre vs 20 min post HFS: Mann-Whitney test, $Tph2^{+/+}$, $n = 7$ cells, $Tph2^{+/GFP}$, $n = 7$ cells, $Tph2^{GFP/GFP}$, $n = 4$ cells: $^{***}P < 0.001$ for all groups $Tph2^{GFP/GFP}$). Either the amplitude and the time course of LTD were similar in these groups as shown in EPSPs traces evoked 10 min before and 20 min after HFS (Fig. 3A, B, right side, one-way ANOVA Bonferroni's multiple comparisons, males, $F_{(2,45)} = 0.80$, $P > 0.05$; $Tph2^{+/+}$ vs $Tph2^{+/GFP}$: $t = 0.36$, $df = 45$; $Tph2^{+/+}$ vs $Tph2^{GFP/GFP}$: $t = 1.23$, $df = 45$; females, $F_{(2,45)} = 1.20$, $P > 0.05$; $Tph2^{+/+}$ vs $Tph2^{+/GFP}$: $t = 1.53$, $df = 45$; $Tph2^{+/+}$ vs $Tph2^{GFP/GFP}$: $t = 0.96$, $df = 45$), suggesting that the mechanisms regulating this form of synaptic plasticity are very similar in both sexes.

In view of the evidence supporting the relevant interaction between DA (Centonze et al., 1999) and 5-HT (Gu, 2002; Kuo et al., 2016) striatal tone on LTP induction, here we have investigated LTP in mice with different *Tph2* gene dosage (Male mice: $Tph2^{+/+}$ $n = 7$, $Tph2^{+/GFP}$ $n = 3$, $Tph2^{GFP/GFP}$ $n = 3$; Female mice: $Tph2^{+/+}$ $n = 6$, $Tph2^{+/GFP}$ $n = 6$, $Tph2^{GFP/GFP}$ $n = 4$).

The application of a HFS protocol was able to induce a long-term enhancement of synaptic transmission (LTP) in SPNs recorded by $Tph2^{+/+}$ and $Tph2^{+/GFP}$ mice, both male and female (Fig. 4A, B). Conversely, LTP was found to be affected in $Tph2^{GFP/GFP}$ mice; in particular this form of plasticity was abolished in males (Fig. 4A; two-way ANOVA: time interaction x genotypes $F_{(30,330)} = 5.97$, males: $Tph2^{+/+}$, $n = 14$ cells, vs $Tph2^{GFP/GFP}$, $n = 3$ cells, and $Tph2^{+/GFP}$, $n = 8$ cells, vs $Tph2^{GFP/GFP}$, $n = 3$ cells, Bonferroni post-hoc $^{###}P < 0.001$) and

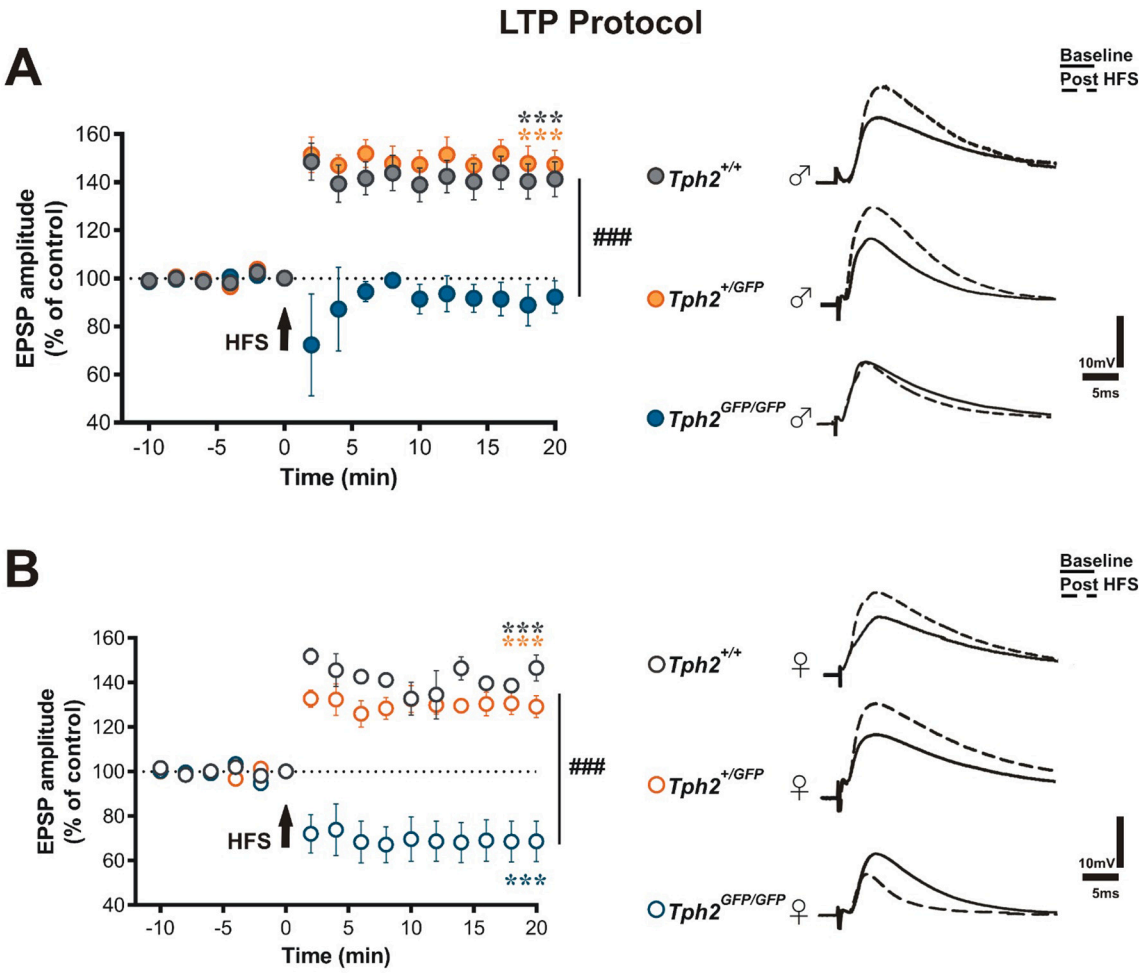

Fig. 4. Long Term Potentiation (LTP) is absent in $Tph2^{GFP/GFP}$ mice. A) Time-course plots of EPSP amplitude (left) and pairs of traces (right) show the absence of HFS-induced LTP in SPNs recorded from $Tph2^{GFP/GFP}$ males mice compared to $Tph2^{+/+}$, $n = 14$ cells, and $Tph2^{+/GFP}$, $n = 8$ cells (two-way ANOVA: time interaction × *genotypes* $F_{(30,330)} = 5.97$, Bonferroni post-hoc $^{###}P < 0.001$ between $Tph2^{+/+}$ vs $Tph2^{GFP/GFP}$, $n = 3$ cells, males, and $Tph2^{+/GFP}$ vs $Tph2^{GFP/GFP}$ males). $Tph2^{+/GFP}$ mice express a normal LTP after tetanic stimulation ($Tph2^{+/+}$, $n = 14$ cells, $Tph2^{+/GFP}$, $n = 8$ cells, males, pre vs 20 min post HFS, Mann-Whitney test,$^{***}P < 0.001$ for both groups); B) Time-course plots of EPSP amplitude (left) and pairs of traces (right) demonstrate the shift of HFS-induced LTP into LTD in SPNs recorded from $Tph2^{GFP/GFP}$ females mice compared to $Tph2^{+/+}$ and $Tph2^{+/GFP}$ animals (two-way ANOVA: time interaction x genotypes $F_{(30,285)} = 16$, Bonferroni post-hoc $^{###}P < 0.001$ between $Tph2^{+/+}$ vs $Tph2^{GFP/GFP}$ females, and $Tph2^{+/GFP}$ vs $Tph2^{GFP/GFP}$ females). $Tph2^{+/GFP}$ females mice express a normal LTP after tetanic stimulation ($Tph2^{+/+}$, $n = 10$ cells, $Tph2^{+/GFP}$, $n = 7$ cells, females, pre vs 20 min post HFS, Mann-Whitney test, $^{***}P < 0.001$ for both groups) and a decrease respect to post-EPSP evoked in $Tph2^{GFP/GFP}$ ($n = 5$ cells) females (pre vs 20 min post HFS, Mann-Whitney test, $^{***}P < 0.001$).

shifted into an LTD in females of the same genotype (Fig. 4B; two-way ANOVA: time interaction x genotypes $F_{(30,285)} = 16$, females: $Tph2^{+/+}$, $n = 10$ cells, vs $Tph2^{GFP/GFP}$, $n = 5$ cells, and $Tph2^{+/GFP}$, $n = 7$ cells vs $Tph2^{GFP/GFP}$, $n = 5$ cells, Bonferroni post-hoc $^{###}P < 0.001$). Relative to the time course and the pairs of traces there was an increase in post-tetanic EPSP amplitude respect to the pre-tetanic control in $Tph2^{+/+}$ and $Tph2^{+/GFP}$ (Fig. 4A, $Tph2^{+/+}$ and $Tph2^{+/GFP}$ males, pre vs 20 min post HFS; Mann-Whitney test, $^{***}P < 0.001$ for both groups; Fig. 4B $Tph2^{+/+}$and $Tph2^{+/GFP}$ females, pre vs 20 min post HFS, Mann-Whitney test, $^{***}P < 0.001$ for both groups) and a decrease respect to post-EPSP evoked in $Tph2^{GFP/GFP}$ females (Fig. 4B, $Tph2^{GFP/GFP}$ females, pre vs 20 min post HFS; Mann-Whitney test, $^{***}P < 0.001$; $Tph2^{GFP/GFP}$ males, pre vs 20 min post HFS; Mann-Whitney test, $P > 0.05$).

3.5. Loss of depotentiation in female $Tph2^{+/GFP}$ mice

We then focused on the analysis of bidirectional synaptic plasticity by the application of a LFS protocol. This mechanism of downscaling of LTP named "depotentiation", increases the efficiency of information storage in neuronal networks and can be involved in the mechanisms underlying extinction in physiological conditions (Ghiglieri et al., 2015; Martella et al., 2009; Picconi et al., 2003).

The most evident difference between $Tph2^{+/+}$ and $Tph2^{+/GFP}$ mice concerns the expression of depotentiation in female mice. In fact, while (as shown in Fig. 4A) we have observed in $Tph2^{+/+}$ males and females a significant depotentiation of the EPSP to the control values 10 min after LTP induction (Fig. 5A, males: $Tph2^{+/+} = 4$ mice, $n = 7$ cells, 10 min LTP vs 10 min after LFS, Mann-Whitney test, $^{\$\$\$}P < 0.001$; females: $Tph2^{+/+} = 4$ mice, $n = 4$ cells, 10 min LTP vs 10 min after LFS, Mann-Whitney test, $^{\$\$}P < 0.01$), the graph in Fig. 5B shows that $Tph2^{+/GFP}$ ($n = 4$ mice) females have lost this physiological mechanism of downscaling useful to restart the synaptic activity of the neuron, opposite to the males ($n = 4$ mice) ($Tph2^{+/GFP}$ female, $n = 5$ cells, 10 min LTP vs 10 min after LFS, $P > 0.05$; $Tph2^{+/GFP}$ males, $n = 5$ cells, 10 min LTP vs 10 min after LFS, Mann-Whitney test, $^{\$\$\$}P < 0.001$).

3.6. 6-OHDA lesion prevents Long Term Depression in $Tph2^{+/GFP}$ mice but not synaptic plasticity in $Tph2^{+/+}$ mice

To study the implication of serotonergic system in modulation of the

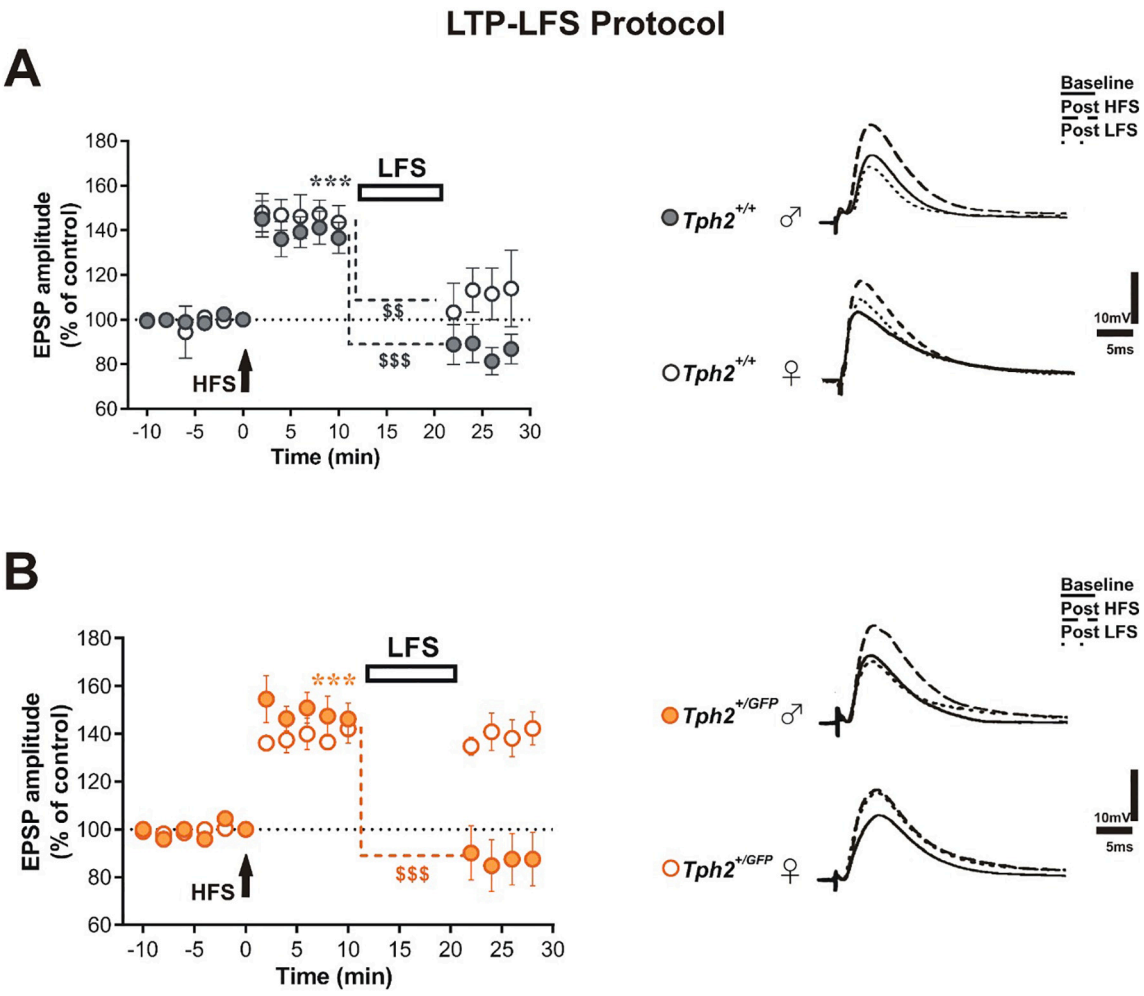

Fig. 5. Low Frequency Stimulation (LFS) protocol did not induce synaptic depotentiation in *Tph2*$^{+/GFP}$ female group. A) LFS of corticostriatal fibers was able to induce depotentiation in all the recorded neurons of control mice, (*Tph2*$^{+/+}$ males, $n = 7$ cells, 10 min LTP vs10 min after LFS, Mann-Whitney test, $^{\$\$\$}P < 0.001$, *Tph2*$^{+/+}$ females, $n = 4$ cells, 10 min LTP vs 10 min after LFS, Mann-Whitney test, $^{\$\$}P < 0.01$); B) HFS was able to induce LTP in both males and females while the LFS protocol induced depotentiation only in male mice (*Tph2*$^{+/GFP}$ males, $n = 5$ cells, 10 min LTP vs 10 min after LFS, Mann-Whitney test, $^{\$\$\$}P < 0.001$). *Tph2*$^{+/GFP}$ female group ($n = 5$ cells), did not show this form of plasticity.

synaptic activity in a pathological condition depleted of DA, we made a partial lesion by injecting 6-OHDA intra-striatum of *Tph2*$^{+/+}$ and *Tph2*$^{+/GFP}$ mice (*Tph2*$^{+/+}$ $n = 3$ mice and *Tph2*$^{+/GFP}$ $n = 3$ mice, both sexes). The low rate survival of *Tph2*$^{GFP/GFP}$ mice after partial dopaminergic denervation (20% of survival after 10 days surgery, Fig. 6A) prevented the inclusion of this cohort in this characterization. In order to confirm the degree of the lesion in *Tph2*$^{+/+}$ ($n = 4$) and *Tph2*$^{+/GFP}$ ($n = 4$) mice, we evaluated the extent of striatal dopaminergic fibers degeneration by immunofluorescence staining of TH (Fig. 6B, one-way ANOVA, $F_{(2,13)} = 10.11$, $P = 0.0023$, Contralateral vs Ipsilateral *Tph2*$^{+/+}$, $^{*}P = 0.0112$; Contralateral vs Ipsilateral *Tph2*$^{+/GFP}$, $^{**}P = 0.0051$; Ipsilateral *Tph2*$^{+/+}$ vs *Tph2*$^{+/GFP}$, *ns* $P = 0.9296$; Contralateral *Tph2*$^{+/GFP}$ vs Contralateral *Tph2*$^{+/+}$ were not statistically significant and were included in the same control group).

The investigation of possible differences in the alterations of SPNs intrinsic membrane properties between the two genotypes has not shown significant changes in membrane potential at rest (*Tph2*$^{+/+}$, -85.82 ± 1.43 mV; *Tph2*$^{+/GFP}$, -88.42 ± 1.09 mV), in mean number of spikes (*Tph2*$^{+/+}$, $n = 5$ cells, 16.60 ± 0.51; *Tph2*$^{+/GFP}$, $n = 4$ cells, 15.25 ± 0.63) and in the I-V curve between SPNs recorded from *Tph2*$^{+/+}$ ($n = 7$ cells) and *Tph2*$^{+/GFP}$ ($n = 9$ cells) (Fig. 6D, two-way ANOVA, time interaction x genotypes $F_{(6,86)} = 1.53$, *Tph2*$^{+/+}$ vs *Tph2*$^{+/GFP}$, $P > 0.05$; Fig. 6E, Students' *t*-test, *Tph2*$^{+/+}$ vs *Tph2*$^{+/GFP}$: $t = 1.68$, $df = 7$, $P > 0.05$). Once the equal response of the neurons of the two genotypes has been ascertained, we analyzed in the partially DA-depleted mice a striatal synaptic plasticity form, which is less conditioned by DA content, i.e. LTD (Fig. 6F). The stimulation protocol of the corticostriatal terminals allowed to check if this form of plasticity is preserved or not in different *Tph2* gene dosages. While in *Tph2*$^{+/+}$ mice lesioned with 6-OHDA ($n = 3$ mice), the HFS was able to induce a normal LTD, this form of plasticity was absent in DA-denervated *Tph2*$^{+/GFP}$ animals ($n = 3$ mice) (Fig. 6F, *Tph2*$^{+/+}$, $n = 4$ cells, pre vs 20 min post HFS, Mann-Whitney test, $^{***}P < 0.001$; *Tph2*$^{+/GFP}$, $n = 5$ cells, pre vs 20 min post HFS, Mann-Whitney test, $P > 0.05$). A significant difference interaction in time between the two experimental groups was appreciable (Fig. 6F, two-way ANOVA: time interaction x genotypes, $F_{(15,105)} = 8.80$, Bonferroni post-hoc, $^{\#\#\#}P < 0.001$).

These results showed the relevant contribution of the serotonergic system to LTD induction in SPNs: a partial reduction of DA content did not interfere with the normal LTD induction in control mice. Conversely, the partial dopaminergic content, coupled with an altered *Tph2* gene dosage, abolished this form of synaptic plasticity in *Tph2*$^{+/GFP}$ mice.

4. Discussion

The main purpose of this study is to explore the influence of 5-HT

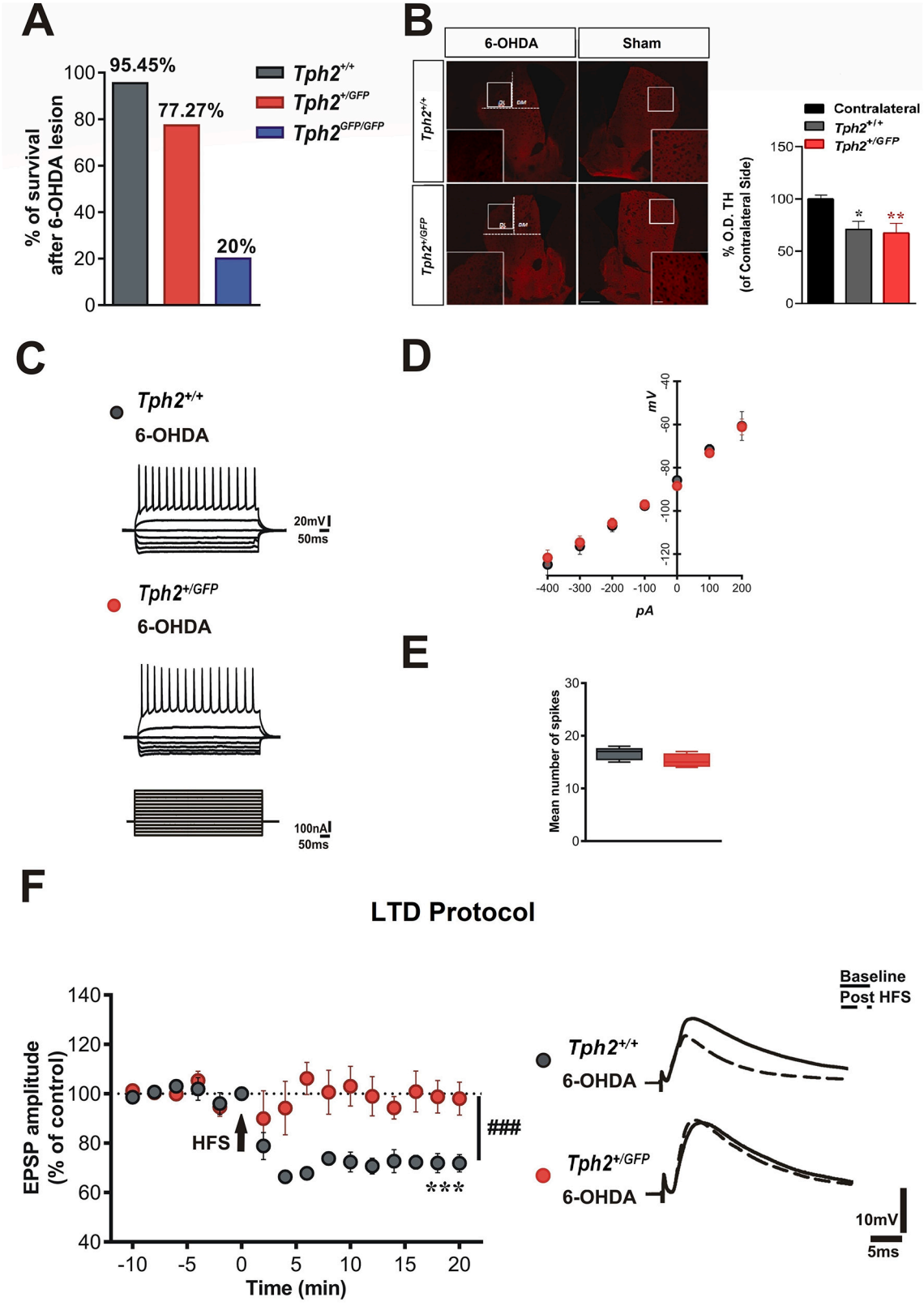

(caption on next page)

Fig. 6. Loss of Long Term Depression (LTD) in *Tph2*$^{+/GFP}$ mice partially-lesioned with 6-OHDA intrastriatum. A) Bar graph shows the percentage of survival in the three genotypes after a partial lesion with 6-OHDA in the dorsolateral (DL) striatum. B) Representative images of TH staining in DL striatum of *Tph2*$^{+/+}$ and *Tph2*$^{+/GFP}$ 6-OHDA mice, showing TH depletion after dopaminergic lesion. LARGE IMAGE 6 × 6 Acquisition, 20× objective, Nikon Confocal Microscope NIKON TiE2, scale bar 500 μm. The Insets show higher magnification images (20× objective) (scale bar 100 μm) of the DL striatum. The graph shows the optical density of TH^{+} fibers (expressed as percentage compared to the Contralateral side), in the Ipsilateral side of *Tph2*$^{+/+}$ or *Tph2*$^{+/GFP}$ in the DL striatum region. Data were expressed as mean ± SEM and analyzed by a one-way ANOVA (one-way ANOVA, $F_{(2,13)} = 10.11$, $P = 0.0023$, Contralateral vs Ipsilateral *Tph2*$^{+/+}$, $^{*}P = 0.0112$; Contralateral vs Ipsilateral *Tph2*$^{+/GFP}$, $^{**}P = 0.0051$; Ipsilateral *Tph2*$^{+/+}$ vs *Tph2*$^{+/GFP}$, *ns* $P = 0.9296$; Contralateral *Tph2*$^{+/GFP}$ vs Contralateral *Tph2*$^{+/+}$ were not statistically significant and were included in the same control group). C) Firing traces of SPNs recorded from *Tph2*$^{+/+}$ 6-OHDA ($n = 7$ cells) and for *Tph2*$^{+/GFP}$ 6-OHDA ($n = 9$ cells) mice. D) Current-voltage (I-V) curves of SPNs the two experimental groups, *Tph2*$^{+/+}$ and *Tph2*$^{+/GFP}$ 6-OHDA mice. E) Comparative graph of the mean number of spikes showing the various *Tph2*$^{+/+}$ and *Tph2*$^{+/GFP}$ 6-OHDA groups. F) LTD is absent in partially 5-HT-depleted mice (*Tph2*$^{+/GFP}$ 6-OHDA). Time-course plots of EPSP amplitude (left) and pairs of traces (right) show that HFS of corticostriatal fibers was able to induce persistent LTD of evoked EPSP only in *Tph2*$^{+/+}$ 6-OHDA mice ($n = 4$ cells) (pre vs 20 min post-HFS, Mann-Whitney test, $^{***}P < 0.001$). There is a post-tetanus interaction of different significance in time between the two experimental groups (two-way ANOVA: time interaction x genotypes $F_{(15,105)} = 8.80$, post-hoc Bonferroni, $^{\#\#\#}P < 0.001$).

transmission on striatal synaptic plasticity. To this aim, we used the *Tph2*^{GFP} knock-in allele that shows selective loss of normal *Tph2* gene expression, despite the presence of an intact serotonergic innervation within the dorsolateral striatum (Migliarini et al., 2013). In addition, the experiments in the parkinsonian 6-OHDA model are aimed at understanding the involvement of the serotonergic system in a DA-denervated pathological state such as Parkinson's disease.

Different findings have shown a possible influence of the serotonergic signaling on corticostriatal synaptic transmission and plasticity (Lesch and Waider, 2012; Mathur et al., 2011). Mathur and collaborators demonstrated that the in vitro application of 5-HT was able to induce a pharmacological LTD of the corticostriatal glutamatergic transmission, suggesting an influence of this monoamine on the plastic changes occurring in striatal neurons (Lesch and Waider, 2012; Mathur et al., 2011).

Based on this observation and consistent with the knowledge that 5-HT transmission in the CNS differs between sexes (Bethea et al., 1996; Bethea et al., 2002; Carlsson and Carlsson, 1988; Lu et al., 1999; Paredes et al., 2019), here we explored the still unclear role of 5-HT in regulating DA-and glutamate-dependent striatal transmission (sEPSC events) and synaptic plasticity (LTD and LTP) in male and females *Tph2*^{GFP} different genotypes.

As previous studies showed that the density and organization of serotonergic fibers in several brain districts, such as the hippocampus, may result altered as a consequence of 5-HT deregulation (Migliarini et al., 2013; Nazzi et al., 2019), we analyzed 5-HT innervation in the striatum using two distinct approaches to identify potential abnormalities. The density of SERT immunoreactive 5-HT fibers in the striatum resulted comparable among the three genotypes Tph2$^{+/+}$, Tph2$^{+/GFP}$ and Tph2$^{GFP/GFP}$ analyzed. In line, the high power 3D fibers reconstruction performed on Tph2$^{+/GFP}$ and Tph2$^{GFP/GFP}$ mice, in which the GFP reporter highlights the 5-HT system (Pratelli et al., 2017), showed that all parameters measured such as total length, mean diameter, occupancy index, and tortuosity of 5-HT fibers were unaffected in mice depleted of brain 5-HT. Taken together, these results demonstrate that in the striatum, 5-HT fibers are not susceptible to 5-HT fluctuations as they appear indistinguishable among the three genotypes, suggesting that the electrophysiological alterations observed in *Tph2* mutant mice are not caused by morphological rearrangements of 5-HT terminals.

The second step of our study was the analysis of spontaneous glutamatergic transmission in the three genotypes. An interesting study published by Pasqualetti's group (Maddaloni et al., 2018) demonstrated in *Tph2*$^{GFP/GFP}$ mutant mice in vivo hyperactive hippocampal transmission and in vitro LTP occlusion. Many studies identified the raphe neurons as a possible additional glutamatergic source within the striatum. This could be hypothesized by the evidence of 5-HT neurons immunoreactivity for glutamate and VGLUT3 (Gras et al., 2002; Nicholas et al., 1992; Ottersen and Storm-Mathisen, 1984) and by the presence of phosphate-activated glutaminase (Kaneko et al., 1990). In addition, Okaty and collaborators in 2015 showed, by the use of a transcriptomics approach, the presence of VGLUT3 RNA in serotonergic neurons (Okaty et al., 2015). In the very recent article published in Cell Reports by Wang and collaborators (Wang et al., 2019) the authors show that co-release is present and, in the case of 5-HT fibers, on ventral tegmental area (VTA) dopaminergic neurons, it is critical for the activation of meso-accumbal neurons. In light of these results, it could be hypothesized a similar control also in the substantia nigra pars compacta.

A limit of this study is that we were not able to study the release of glutamate from serotonergic neurons that would provide a dissection of its role on the observed changes in plasticity. However, consistent with a role of serotonergic signaling in the modulation of striatal transmission at SPNs (Fornal et al., 1996), we can hypothesize that the increased amplitude of sEPSC, recorded in SPNs of *Tph2*$^{GFP/GFP}$ mutants, may result from a loss of autoinhibitory effect regulated by 5-HT with the consequent net increase of glutamate-mediated responses. Interestingly, these results may partially explain our finding of an impaired LTP in mutant male and female mice; in fact, this form of synaptic plasticity is altered in the case of increased EPSPs amplitude resulting from changes in glutamatergic transmission. We observed that LTD was completely preserved in all experimental groups (*Tph2*$^{+/+}$, *Tph2*$^{+/GFP}$ and *Tph2*$^{GFP/GFP}$ male and female mice) (Fig. 2A, B), highlighting that 5-HT is not involved in regulating this form of striatal synaptic plasticity.

The analysis of LTP induction in *Tph2*^{GFP} mice (Fig. 4A, B) unveils a 5-HT modulation of this form of synaptic plasticity. Indeed, *Tph2*$^{+/GFP}$ male and female mice express LTP with amplitude and time course identical to those seen in the control group, while in *Tph2*$^{GFP/GFP}$ male mice we found a loss of LTP (Fig. 4A, light blue symbols), and in *Tph2*$^{GFP/GFP}$ female mice the loss of this form of plasticity unmasks a synaptic depression (Fig. 4B, light blue symbols). In view of the knowledge that DA has a primary role in the induction of striatal LTP, the absence of potentiation in *Tph2*$^{GFP/GFP}$ mice might support the idea of a functional implication of serotonergic transmission together with DA in regulating striatal LTP.

Notably, our finding reveals a form of metaplasticity in female *Tph2*$^{GFP/GFP}$ mice (LTP shift toward LTD), which might be of great importance to understand the role of altered 5-HT homeostasis within the striatal nucleus. In addition, females *Tph2*$^{+/GFP}$ were characterized by a loss of depotentiation of previously induced LTP (Fig. 5B, orange empty symbols) compared to a normal bidirectional synaptic plasticity observed in male mice (Fig. 5A, grey empty symbols).

Taken together, these data show that *Tph2* gene dosage exerts a primary role in modulating bidirectional synaptic plasticity in a sex-sensitive manner.

Furthermore, we investigated how the striatal synaptic plasticity can be modified when both the serotonergic and dopaminergic systems are compromised. As previously demonstrated, a partial dopaminergic lesion in mice and rats does not abolish LTD, requiring low levels of DA, while it blocks LTP induction, which requires higher concentrations of this neurotransmitter (Paille et al., 2010; Picconi et al., 2003).

Electrophysiological recordings of SPNs showed a normally expressed LTD in 6-OHDA-partially lesioned striatum of *Tph2*$^{+/+}$ mice (Fig. 6), while the SPNs recorded from the 6-OHDA-partially lesioned *Tph2*$^{+/GFP}$ could not express this form of plasticity. These results suggest

that functional interaction between the serotonergic and dopaminergic systems in the induction of striatal plasticity, already demonstrated in physiological and in pathological states (Carta et al., 2007; Lesch and Waider, 2012; Mathur et al., 2011), also exists in the two conditions of 5-HT depletion alone and combined with DA depletion. In *Tph2*$^{GFP/GFP}$, the complete lack of 5-HT and the partial depletion of DA are responsible for a lower survival rate. This indicates that in the absence of 5-HT, even a partial DA denervation compromises the homeostatic processes needed for brain functions.

This study performed in *Tph2*^{GFP} mice sets the basis to understand the essential influence of serotonergic transmission on the regulation of striatal glutamatergic synapse function. In addition, for the first time, the role of 5-HT and DA interaction emerge in striatal dependent synaptic plasticity in the two sexes.

Declaration of competing interest

No conflicts of interest, financial or otherwise, are declared by the authors.

Acknowledgments

This work was supported by the Italian Ministry of Health, Ricerca finalizzata-RF-2013-02357386 (to A.U., B.P., M.P.) and Ricerca Corrente and by PRA-2018 from University of Pisa to M.P.

References

Alenina, N., et al., 2009. Growth retardation and altered autonomic control in mice lacking brain serotonin. Proc. Natl. Acad. Sci. U. S. A. 106, 10332–10337.
Bagetta, V., et al., 2012. Rebalance of striatal NMDA/AMPA receptor ratio underlies the reduced emergence of dyskinesia during D2-like dopamine agonist treatment in experimental Parkinson's disease. J. Neurosci. 32, 17921–17931.
Bethea, C.L., et al., 1996. Steroid regulation of estrogen and progestin receptor messenger ribonucleic acid in monkey hypothalamus and pituitary. Endocrinology 137, 4372–4383.
Bethea, C.L., et al., 2002. Diverse actions of ovarian steroids in the serotonin neural system. Front. Neuroendocrinol. 23, 41–100.
Byers, S.L., et al., 2012. Mouse estrous cycle identification tool and images. PLoS One 7, e35538.
Calabresi, P., et al., 1992. Long-term potentiation in the striatum is unmasked by removing the voltage-dependent magnesium block of NMDA receptor channels. Eur. J. Neurosci. 4, 929–935.
Carli, M., et al., 2015. Tph2 gene deletion enhances amphetamine-induced hypermotility: effect of 5-HT restoration and role of striatal noradrenaline release. J. Neurochem. 135, 674–685.
Carlsson, M., Carlsson, A., 1988. A regional study of sex differences in rat brain serotonin. Prog. Neuro-Psychopharmacol. Biol. Psychiatry 12, 53–61.
Carta, M., et al., 2007. Dopamine released from 5-HT terminals is the cause of L-DOPA-induced dyskinesia in parkinsonian rats. Brain 130, 1819–1833.
Cavaccini, A., et al., 2018. Serotonergic signaling controls input-specific synaptic plasticity at striatal circuits. Neuron 98, 801–816.e7.
Centonze, D., et al., 1999. Unilateral dopamine denervation blocks corticostriatal LTP. J. Neurophysiol. 82, 3575–3579.
Cerovic, M., et al., 2015. Derangement of Ras-guanine nucleotide-releasing factor 1 (Ras-GRF1) and extracellular signal-regulated kinase (ERK) dependent striatal plasticity in L-DOPA-induced dyskinesia. Biol. Psychiatry 77, 106–115.
Cervo, L., et al., 2005. Genotype-dependent activity of tryptophan hydroxylase-2 determines the response to citalopram in a mouse model of depression. J. Neurosci. 25, 8165–8172.
De Deurwaerdere, P., Di Giovanni, G., 2017. Serotonergic modulation of the activity of mesencephalic dopaminergic systems: therapeutic implications. Prog. Neurobiol. 151, 175–236.
Duman, R.S., et al., 2016. Synaptic plasticity and depression: new insights from stress and rapid-acting antidepressants. Nat. Med. 22, 238–249.
Fornal, C.A., et al., 1996. A subgroup of dorsal raphe serotonergic neurons in the cat is strongly activated during oral-buccal movements. Brain Res. 716, 123–133.
Ghiglieri, V., et al., 2015. Rhes influences striatal cAMP/PKA-dependent signaling and synaptic plasticity in a gender-sensitive fashion. Sci. Rep. 5, 10933.
Gras, C., et al., 2002. A third vesicular glutamate transporter expressed by cholinergic and serotoninergic neurons. J. Neurosci. 22, 5442–5451.
Gu, Q., 2002. Neuromodulatory transmitter systems in the cortex and their role in cortical plasticity. Neuroscience 111, 815–835.
Heiming, R.S., et al., 2009. Living in a dangerous world: the shaping of behavioral profile by early environment and 5-HTT genotype. Front. Behav. Neurosci. 3, 26.
Kaneko, T., et al., 1990. Immunohistochemical demonstration of glutaminase in catecholaminergic and serotoninergic neurons of rat brain. Brain Res. 507, 151–154.
Kuo, H.I., et al., 2016. Chronic enhancement of serotonin facilitates excitatory transcranial direct current stimulation-induced neuroplasticity. Neuropsychopharmacology 41, 1223–1230.
Lesch, K.P., Waider, J., 2012. Serotonin in the modulation of neural plasticity and networks: implications for neurodevelopmental disorders. Neuron 76, 175–191.
Lu, N.Z., et al., 1999. Ovarian steroid action on tryptophan hydroxylase protein and serotonin compared to localization of ovarian steroid receptors in midbrain of guinea pigs. Endocrine 11, 257–267.
Lundblad, M., et al., 2004. A model of L-DOPA-induced dyskinesia in 6-hydroxydopamine lesioned mice: relation to motor and cellular parameters of nigrostriatal function. Neurobiol. Dis. 16, 110–123.
Maddaloni, G., et al., 2017. Development of serotonergic fibers in the post-natal mouse brain. Front. Cell. Neurosci. 11, 202.
Maddaloni, G., et al., 2018. Serotonin depletion causes valproate-responsive manic-like condition and increased hippocampal neuroplasticity that are reversed by stress. Sci. Rep. 8, 11847.
Martella, G., et al., 2009. Impairment of bidirectional synaptic plasticity in the striatum of a mouse model of DYT1 dystonia: role of endogenous acetylcholine. Brain 132, 2336–2349.
Mathur, B.N., et al., 2011. Serotonin induces long-term depression at corticostriatal synapses. J. Neurosci. 31, 7402–7411.
Migliarini, S., et al., 2013. Lack of brain serotonin affects postnatal development and serotonergic neuronal circuitry formation. Mol. Psychiatry 18, 1106–1118.
Nazzi, S., et al., 2019. Fluoxetine induces morphological rearrangements of serotonergic fibers in the hippocampus. ACS Chem. Neurosci. 10, 3218–3224.
Nicholas, A.P., et al., 1992. Serotonin-, substance P- and glutamate/aspartate-like immunoreactivities in medullo-spinal pathways of rat and primate. Neuroscience 48, 545–559.
Ogawa, S.K., Watabe-Uchida, M., 2018. Organization of dopamine and serotonin system: anatomical and functional mapping of monosynaptic inputs using rabies virus. Pharmacol. Biochem. Behav. 174, 9–22.
Okaty, B.W., et al., 2015. Multi-scale molecular deconstruction of the serotonin neuron system. Neuron 88, 774–791.
Ottersen, O.P., Storm-Mathisen, J., 1984. Glutamate- and GABA-containing neurons in the mouse and rat brain, as demonstrated with a new immunocytochemical technique. J. Comp. Neurol. 229, 374–392.
Paille, V., et al., 2010. Distinct levels of dopamine denervation differentially alter striatal synaptic plasticity and NMDA receptor subunit composition. J. Neurosci. 30, 14182–14193.
Paredes, S., et al., 2019. An association of serotonin with pain disorders and its modulation by estrogens. Int. J. Mol. Sci. 20.
Picconi, B., et al., 2003. Loss of bidirectional striatal synaptic plasticity in L-DOPA-induced dyskinesia. Nat. Neurosci. 6, 501–506.
Pratelli, M., Pasqualetti, M., 2019. Serotonergic neurotransmission manipulation for the understanding of brain development and function: learning from Tph2 genetic models. Biochimie 161, 3–14.
Pratelli, M., et al., 2017. Perturbation of serotonin homeostasis during adulthood affects serotonergic neuronal circuitry. eNeuro 4.
Schindelin, J., et al., 2012. Fiji: an open-source platform for biological-image analysis. Nat. Methods 9, 676–682.
Svob Strac, D., et al., 2016. The serotonergic system and cognitive function. Transl. Neurosci. 7, 35–49.
Trudeau, L.E., 2004. Glutamate co-transmission as an emerging concept in monoamine neuron function. J. Psychiatry Neurosci. 29, 296–310.
Wang, H.L., et al., 2019. Dorsal raphe dual serotonin-glutamate neurons drive reward by establishing excitatory synapses on VTA mesoaccumbens dopamine neurons. Cell Rep. 26, 1128–1142.e7.
Zhang, X., et al., 2004. Tryptophan hydroxylase-2 controls brain serotonin synthesis. Science 305, 217.